Journal of Power Sources 183 (2008) 581–585

Contents lists available at ScienceDirect

Journal of Power Sources

journal homepage: www.elsevier.com/locate/jpowsour

Short communication

Characterization of $Pr_{1-x}Sr_xCo_{0.8}Fe_{0.2}O_{3-\delta}$ ($0.2 \leq x \leq 0.6$) cathode materials for intermediate-temperature solid oxide fuel cells

Xiangwei Meng, Shiquan Lü, Yuan Ji*, Tao Wei, Yanlei Zhang

College of Physics, Jilin University, Changchun 130023, PR China

ARTICLE INFO

Article history:
Received 16 April 2008
Received in revised form 20 May 2008
Accepted 21 May 2008
Available online 27 May 2008

Keywords:
Cathode
Intermediate-temperature solid oxide fuel cells
Electrical conductivities
Interfacial impedance

ABSTRACT

Cathode materials consisting of $Pr_{1-x}Sr_xCo_{0.8}Fe_{0.2}O_{3-\delta}$ ($x = 0.2$–0.6) were prepared by the sol–gel process for intermediate-temperature solid oxide fuel cells (IT-SOFCs). The samples had an orthorhombic perovskite structure. The electrical conductivities were all higher than 279 S cm^{-1}. The highest conductivity, 1040 S cm^{-1}, was found at 300 °C for the composition $x = 0.4$. Symmetrical cathodes made of $Pr_{0.6}Sr_{0.4}Co_{0.8}Fe_{0.2}O_{3-\delta}$ (PSCF)–$Ce_{0.85}Gd_{0.15}O_{1.925}$ (50:50 by weight) composite powders were screen-printed on GDC electrolyte pellets. The area specific resistance value for the PSCF–GDC cathode was as low as 0.046 Ω cm^2 at 800 °C. The maximum power densities of a cell using the PSCF–GDC cathode were 520 mW cm^{-2}, 435 mW cm^{-2} and 303 mW cm^{-2} at 800 °C, 750 °C and 700 °C, respectively.

1. Introduction

A solid oxide fuel cell (SOFC) is an energy-conversion system of great industrial interest because of its high-energy efficiency and environmental advantages [1]. However, the necessity for high operating temperatures (800–1000 °C) has resulted in challenges concerning materials compatibility and high costs [2]. In recent years, the focus of the SOFC is shifting towards operation at intermediate-temperature (IT, 500–800 °C), since lower temperatures can minimize the problems associated with thermal-expansion mismatch and chemical reactivity among the components [3]. Unfortunately, one of the main obstacles is that the cathode resistance increases greatly with decreasing temperature [4].

The traditional cathode material $La_{1-x}Sr_xMnO_3$ (LSM) is deemed to be one of the most promising cathode materials for high-temperature SOFCs because of its outstanding electrochemical performance, thermal and chemical stability and relatively good compatibility with yttria-stabilized zirconia (YSZ) [5,6]. The cathode polarization resistance R_p is smaller than 1 Ω cm^2 at 1000 °C. However, its poor oxide–ion conductivity prevents its use for IT-SOFCs. For example, when the temperature drops to 500 °C, the cathode's electrical conductivity is greatly reduced and the cathode resistance is as high as 2000 Ω cm^2 [7].

In recent years, $Ln_{1-x}Sr_xCo_{1-y}Fe_yO_{3-\delta}$ (Ln = La, Sm, Nd, Gd, Dy) has become the cathode material of choice for IT-SOFCs, because of its high electronic and ionic conductivity as well as its high catalytic activity for oxygen reduction [8]. Its high ionic conductivity enables the oxygen species to migrate through the bulk as well as the surface of the electrode material to the triple-phase boundary (TPB) [9]. The R_p values of the $La_{0.58}Sr_{0.4}Co_{0.2}Fe_{0.8}O_{3-\delta}$–$Ce_{0.8}Sm_{0.2}O_{2-\delta}$ (SDC) cathode on SDC electrolyte were 0.23 Ω cm^2 at 700 °C and 0.067 Ω cm^2 at 750 °C, much lower than the R_p of an LSM cathode on YSZ electrolyte [10]. However, it has a high thermal-expansion coefficient which is mismatched to that of common ITSOFC electrolyte materials [11,12]. $Ln_{1-x}Sr_xCo_{1-y}Fe_yO_{3-\delta}$-based composite electrodes show some improved electrochemical properties, which have been attributed to the contribution of the increased length of the TPB [13]. In addition, composite electrodes can have a decreased thermal-expansion coefficient, which is matched to that of common ITSOFC electrolyte materials.

In this paper, we have fabricated a series of cathodes consisting of $Pr_{1-x}Sr_xCo_{0.8}Fe_{0.2}O_{3-\delta}$ ($x = 0.2$–0.6), and found that the best proportion for IT-SOFCs was $Pr_{0.6}Sr_{0.4}Co_{0.8}Fe_{0.2}O_{3-\delta}$ (PSCF). Subsequently, we manufactured a PSCF–$Ce_{0.85}Gd_{0.15}O_{1.925}$ (GDC) composite cathode. The aim of this study was to investigate the electrochemical properties of the PSCF–GDC composite cathode, and to present and discuss its performance in electrolyte (GDC)-supported cells.

2. Experimental

$Pr_{1-x}Sr_xCo_{0.8}Fe_{0.2}O_{3-\delta}$ ($x = 0.2$–0.6) powders were prepared by the sol–gel method. The appropriate metal nitrates were mixed in distilled water. When they had dissolved completely, a certain

* Corresponding author. Tel.: +86 431 8566 0418; fax: +86 431 8849 8000.
E-mail address: jiyuan@jlu.edu.cn (Y. Ji).

0378-7753/$ – see front matter © 2008 Elsevier B.V. All rights reserved.
doi:10.1016/j.jpowsour.2008.05.052

amount of citric acid was introduced, the mole ratio of citric acid:total metal ions being controlled around 1.2:1. Mild heating induced gelation of the solution; the resulting gel was held in a drying oven at 120 °C for 3 h to remove organics, and then sintered at 900 °C and 1000 °C for 6 h. Powders of GDC were also synthesized using the sol–gel method and firing at 600 °C for 4 h.

Symmetrical electrochemical cells for impedance studies were prepared using a PSCF–GDC (50:50 by weight) composite cathode and GDC electrolyte. The PSCF and GDC powders were mixed fully in ethanol, and slurries were made up with organic solvent. These slurries were screen-printed on each side of a GDC electrolyte pellet. After drying, the samples were sintered at 950 °C, 1000 °C and 1050 °C for 2 h, respectively.

The GDC powder was pressed into a pellet and sintered at 1400 °C for 10 h in air. The composite anode consisting of NiO–35GDC (65:35 by weight) and the PSCF–GDC composite cathode were deposited on each side of the GDC electrolyte disk (0.3 mm thick) by the screen-printing technique. After sintered the anode at 1250 °C for 4 h, the cathode was heat-treated at 1000 °C for 2 h. A single cell was sealed at one end of an alumina tube by applying silver paste. The cathode side was open to air, and the anode side was exposed to H_2 at a flow rate of 10 ml min^{-1}.

The phase of the PSCF powers was identified by powder X-ray diffraction (Rigaku-D-Max Ra system operating at 12 kW with Cu Kα radiation). A JEOL JSM-6480LV scanning electron microscope (SEM) was employed to examine the microstructures of the sintered samples. Electrical conductivity was measured as a function of temperature by the standard dc four-terminal method. The thermal expansion coefficient (TEC) was carried out using a horizontal pushrod dilatometer (Netzsch DIL 402C) with an Al_2O_3 reference

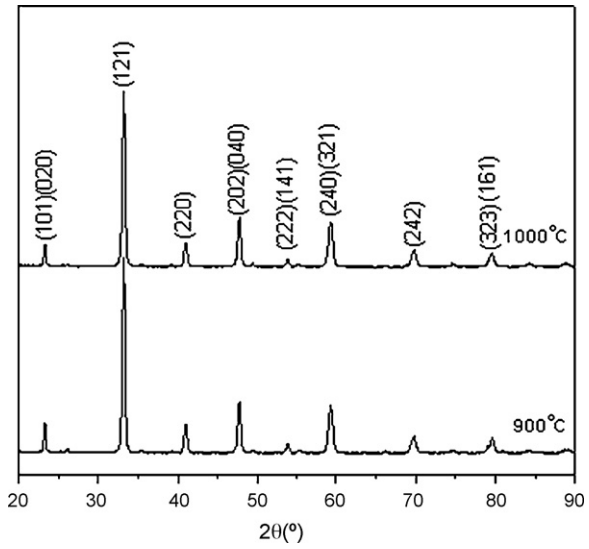

Fig. 1. X-ray diffraction patterns of $Pr_{0.7}Sr_{0.3}Co_{0.8}Fe_{0.2}O_{3-\delta}$.

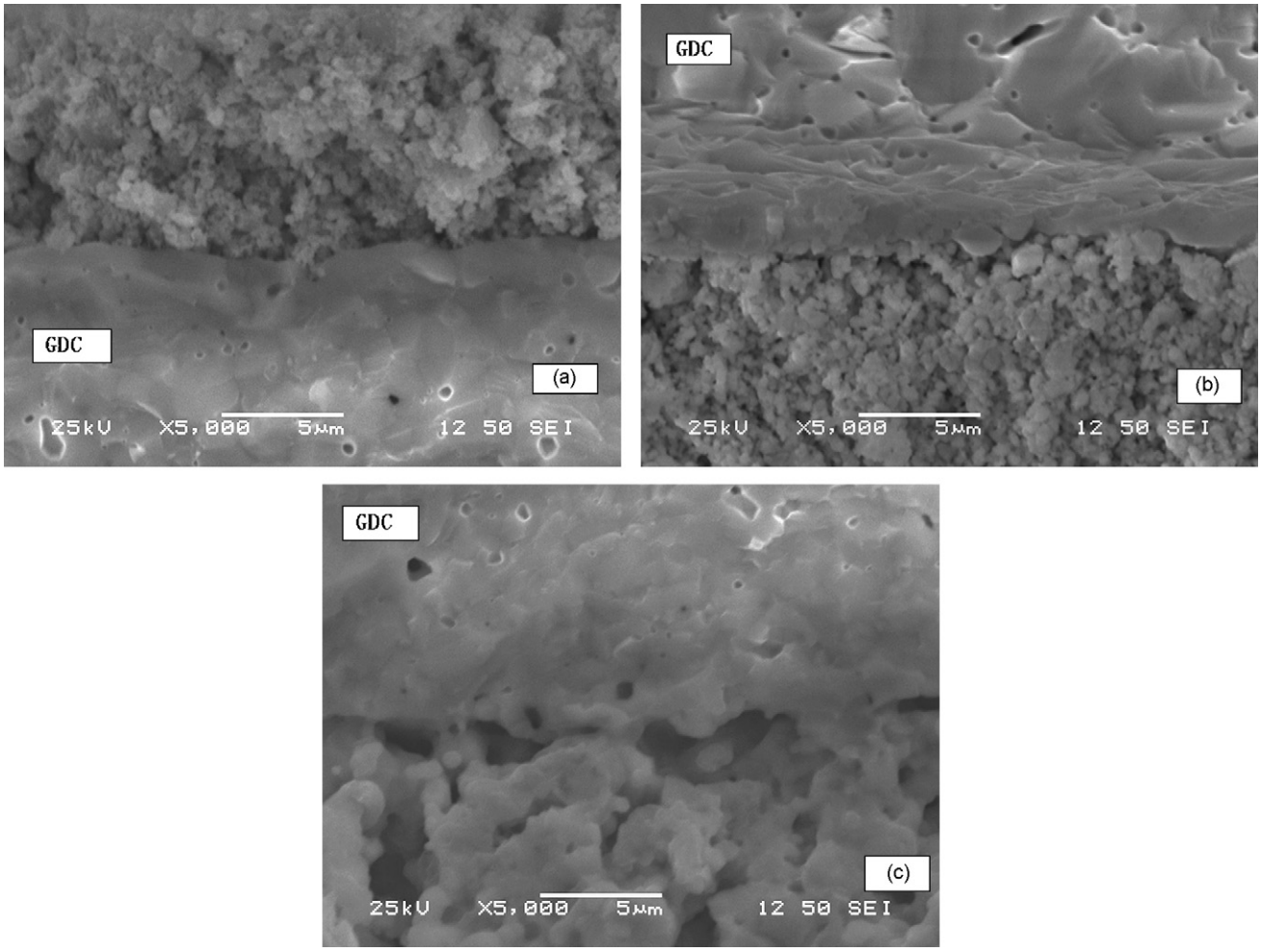

Fig. 2. Cross-sectional SEM micrographs of the fuel cell using $Pr_{0.6}Sr_{0.4}Co_{0.8}Fe_{0.2}O_{3-\delta}$ (PSCF)–GDC composite electrodes sintered at different temperatures: (a) 900 °C, (b) 1000 °C, and (c) 1100 °C.

in the temperature range from 30 to 850 °C with a heating rate at 5 °C min^{-1}. The electrochemical performance was evaluated by a CHI604C analyzer and ac impedance spectroscopy measurements were carried out under open-circuit conditions from 0.01 Hz to 10^5 Hz with a signal amplitude of 10 mV.

3. Results and discussion

3.1. Crystal structure analysis

Fig. 1 shows the XRD patterns of $Pr_{0.7}Sr_{0.3}Co_{0.8}Fe_{0.2}O_{3-\delta}$ powder, which are typical for this series of samples ($Pr_{1-x}Sr_xCo_{0.8}Fe_{0.2}O_{3-\delta}$ (x = 0.2–0.6)). It can be seen that the major peaks are well indexed and almost the same as those of $PrCoO_3$ (PDF card no. 89-8415), showing single orthorhombic perovskite-type structure. From calculations using the XRD data, the lattice parameters a, b, c, for $Pr_{0.7}Sr_{0.3}Co_{0.8}Fe_{0.2}O_{3-\delta}$ are were refined to be 0.5393 nm, 0.7626 nm, 0.5391 nm, respectively. The $Pr_{0.7}Sr_{0.3}Co_{0.8}Fe_{0.2}O_{3-\delta}$ powders prepared using different sintering temperatures (900 °C and 1000 °C for 6 h) exhibited almost the same characteristic peaks, indicating that $Pr_{1-x}Sr_xCo_{0.8}Fe_{0.2}O_{3-\delta}$ (x = 0.2–0.6) with a single-phase orthorhombic perovskite structure could be obtained after sintering at 900 °C.

3.2. Microstructural characteristics

Fig. 2 shows the microstructures of the fractured cells after electrochemical testing.

Different PSCF–GDC (50:50 by weight) composite cathodes (sintered at 900 °C, 1000 °C and 1100 °C for 2 h) were used in the fuel cells. In general, sintering at high-temperature increases the grain size of an electrode, which will decrease the surface area–gas solid interface (TPB) then increase the polarization resistance [10]. On the other hand, due to the increase in the sintering temperature, the electrode particles adhere strongly to the electrolyte surface. Therefore, obtaining PSCF particles with a fine microstructure and ensuring their strong adhesion to the GDC electrolyte are in a trade-off relationship with respect to the sintering temperature. Fig. 2(a) shows that a PSCF–GDC electrode sintered at 900 °C has a smaller grain size but poorer porosity. Fig. 2(c) shows that a PSCF–GDC cathode sintered at 1100 °C has a much larger grain size, which will decrease the TPB. A PSCF–GDC electrode sintered at 1000 °C (Fig. 2(b)) showed a smaller grain size and reasonable porosity to ensure gas diffusion. Also the cathode appeared to be in good contact with the dense electrolyte pellet.

3.3. Electrical conductivity measurements

The temperature dependence of the electrical conductivity for $Pr_{1-x}Sr_xCo_{0.8}Fe_{0.2}O_{3-\delta}$ (x = 0.2–0.6) is shown in Fig. 3. The electrical conductivity values are all higher than 279 S cm^{-1}. The highest conductivity, 1040 S cm^{-1}, is found at 300 °C for the composition x = 0.4. It meets the requirements of an ITSOFC cathode. For the $Pr_{1-x}Sr_xCo_{0.8}Fe_{0.2}O_{3-\delta}$ (x = 0.2, 0.3) sample, the electrical conductivity first increases, goes through a maximum and then decreases with increasing temperature. At temperatures lower than this maximum, the electrical conductivity is found to follow small-polaron semiconducting behavior. The decrease in conductivity after the temperature exceeded this maximum could be due to the loss of oxygen from the lattice at higher temperatures. For the $Pr_{1-x}Sr_xCo_{0.8}Fe_{0.2}O_{3-\delta}$ (x = 0.4–0.6) sample, the electrical conductivity decreases with increasing temperature, implying metallic behavior. The $Pr_{1-x}Sr_xCo_{0.8}Fe_{0.2}O_{3-\delta}$ system exhibits a semiconductor-to-metal transition around x = 0.3. As described previously with the $Nd_{1-x}Sr_xCoO_{3-\delta}$ system [14], the

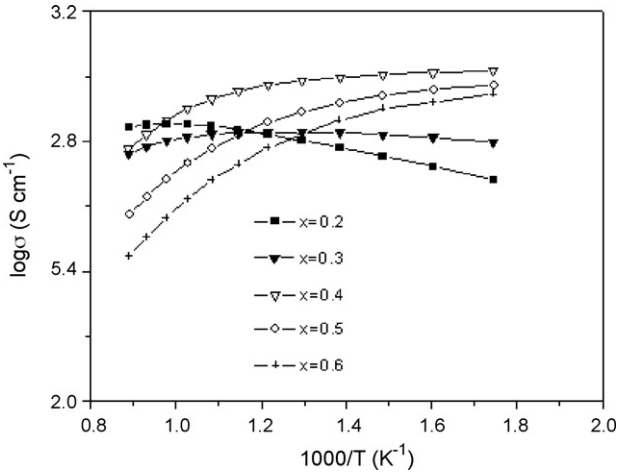

Fig. 3. Temperature dependence of the electrical conductivity for $Pr_{1-x}Sr_xCo_{0.8}Fe_{0.2}O_{3-\delta}$ (x = 0.2–0.6).

semiconductor-to-metal transition in $Pr_{1-x}Sr_xCo_{0.8}Fe_{0.2}O_{3-\delta}$ can also be understood by considering the changes in the structural parameters. The Goldschmidt tolerance factor t can be used as a measure of the deviation of the ABO_3 perovskite structure from ideal cubic symmetry:

$$t = \frac{r_A + r_O}{\sqrt{2}(r_B + r_O)} \quad (1)$$

where r_A, r_B, and r_O are the radii of A^{3+}, B^{3+}, and O^{2-} ions, respectively. Some Fe^{4+} and Co^{4+} will exist as Sr^{2+} is introduced at Pr^{3+} lattice positions because of electronic charge compensation. The value of t will increase because Sr^{2+} (0.144 nm) is larger than Pr^{3+} (0.13 nm) and Co^{4+} (0.053 nm)/Fe^{4+} (0.0585 nm) is smaller than Co^{3+} (0.0545 nm)/Fe^{3+}(0.0645 nm). The increase in the tolerance factor with increasing x in $Pr_{1-x}Sr_xCo_{0.8}Fe_{0.2}O_{3-\delta}$ (x = 0.2–0.6) results in the increasing covalency of the (Co, Fe)–O bonds, with an oxidation of Co^{3+}/Fe^{3+} to Co^{4+}/Fe^{4+}. The consequent increase in the bandwidth and a vanishing of the charge-transfer gap could be envisioned to cause a semiconductor-to-metal transition with increasing x in $Pr_{1-x}Sr_xCo_{0.8}Fe_{0.2}O_{3-\delta}$ (x = 0.2–0.6).

3.4. Thermal expansion

Fig. 4 shows the thermal expansion curves of $Pr_{1-x}Sr_xCo_{0.8}Fe_{0.2}O_{3-\delta}$($x$ = 0.4, 0.6). The average thermal expansion coefficients

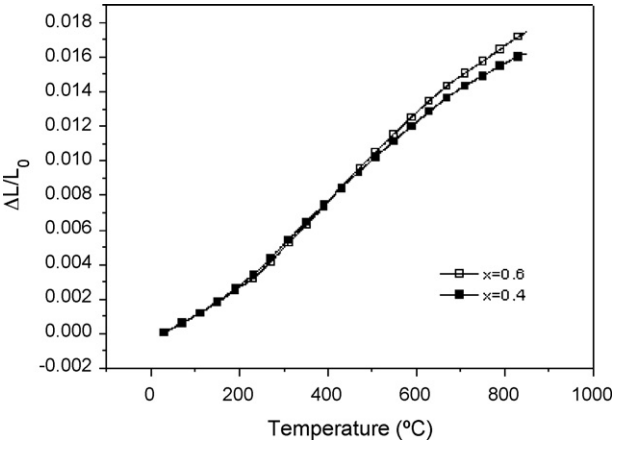

Fig. 4. Thermal expansion curves for $Pr_{1-x}Sr_xCo_{0.8}Fe_{0.2}O_{3-\delta}$ (x = 0.3, 0.4) as a function of temperature.

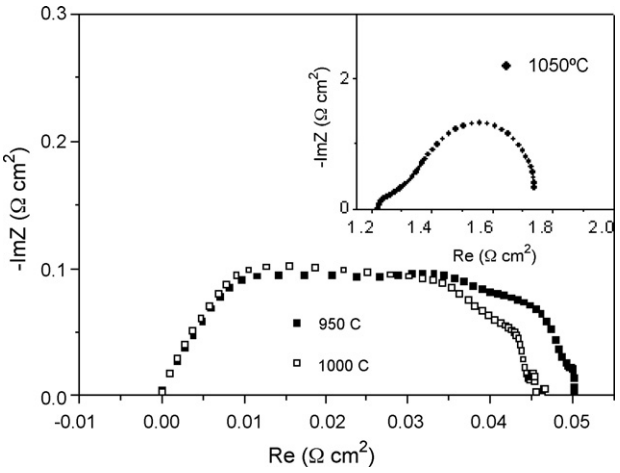

Fig. 5. Impedance spectra of $Pr_{0.6}Sr_{0.4}Co_{0.8}Fe_{0.2}O_{3-\delta}$ (PSCF)–GDC composite cathodes sintered at different temperatures.

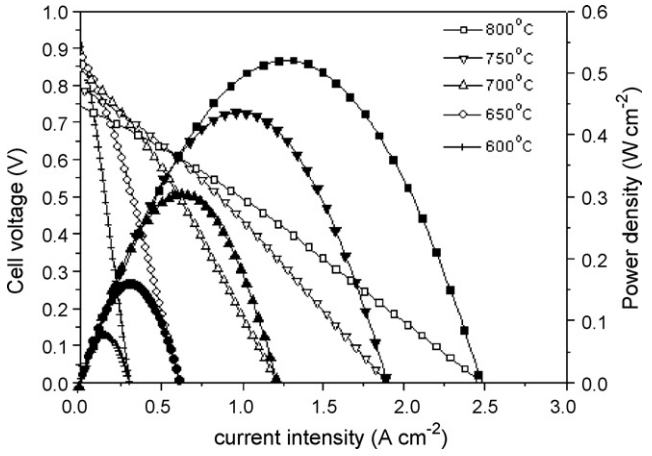

Fig. 6. Cell voltage and power density as functions of current density with $Pr_{0.6}Sr_{0.4}Co_{0.8}Fe_{0.2}O_{3-\delta}$ (PSCF)–GDC composite cathode.

of $Pr_{1-x}Sr_xCo_{0.8}Fe_{0.2}O_{3-\delta}$($x$ = 0.4, 0.6) between 30 °C and 850 °C are about $19.69 \times 10^{-6}\,K^{-1}$ (x = 0.4) and $21.23 \times 10^{-6}\,K^{-1}$ (x = 0.6). The figures were higher than that of GDC electrolyte ($12.56 \times 10^{-6}\,K^{-1}$, measured by our lab). In order to decrease thermal expansion coefficient we fabricated composite electrodes which can match well with GDC electrolyte.

3.5. Impedance analysis

The interfacial impedance spectra for PSCF–GDC (50:50 by weight) composite cathodes fired at 950 °C, 1000 °C and 1050 °C are shown in Fig. 5. Under an open-circuit potential at 800 °C in air, all the spectra consist of two arcs. The ac impedance is made up of both ohmic and interfacial resistances. The intercept with the real axis at high frequencies is the grain (bulk) boundary response of the GDC electrolyte. The arc observed at lower frequency can be associated with the interfacial impedance between the PSCF–GDC composite cathode and the GDC electrolyte. The area specific resistance (ASR) value of PSCF–GDC sintered at 1000 °C on GDC electrolyte is 0.046 Ω cm² at 800 °C, which is much lower than the 0.516 Ω cm² measured at 800 °C for PSCF–GDC sintered at 1050 °C. Its value is a little lower than that of PSCF–GDC sintered at 950 °C, which is 0.05 Ω cm². These results indicate that PSCF–50GDC sintered at 1000 °C has the smallest interfacial resistance as well as the best electrochemical performance at open-circuit potential.

Considering the SEM photos of PSCF–GDC sintered at 1000 °C (Fig. 2(b)), which showed reasonable porosity to ensure gas diffusion and good contact with the dense electrolyte pellet, we think 1000 °C is the appropriate sintering temperature for this composite cathode.

3.6. Cell-performance analysis

Fig. 6 shows the power densities of GDC-supported fuel cells using PSCF–GDC (50:50 by weight, sintered at 1000 °C for 2 h) as the composite cathode and NiO–35GDC (sintered at 1250 °C for 4 h) as the composite anode. The cells were tested at different temperatures (600–800 °C) with hydrogen as fuel and air as oxidant. As can be seen, the power density increases with increasing operating temperature. The maximum power densities of cells with the PSCF–GDC composite cathode are 520 mW cm^{-2}, 435 mW cm^{-2} and 303 mW cm^{-2} at 800 °C, 750 °C and 700 °C, respectively.

In our study, the substitution of a divalent cation (Sr^{2+}) for a trivalent or tetravalent cation in the A-sites gives rise to a relatively high ionic conductivity and excellent mixed ionic–electronic conduction characteristics by the creation of more oxygen vacancies in perovskite oxides [15,16]. A high oxide-vacancy concentration on the electrode surface could improve the dissociation of the O_2 oxygen molecule into atomic oxygen O, increasing the pathway for the diffusion of the reduced oxygen ions [16–18]. At the same time, PSCF–GDC composite cathodes effectively enhance the length of the TPB for the O_2 reduction reaction. Therefore, as a mixed ionic–electronic conductor, the PSCF–GDC composite cathode is a good candidate for operation at or below 800 °C.

4. Conclusions

The physical properties and electrochemical characteristics of $Pr_{1-x}Sr_xCo_{0.8}Fe_{0.2}O_{3-\delta}$ (x = 0.2–0.6) have been investigated. All the samples have a single orthorhombic phase. The electrical conductivities of $Pr_{1-x}Sr_xCo_{0.8}Fe_{0.2}O_{3-\delta}$ (x = 0.2–0.6) are all higher than 279 S cm^{-1}. The highest conductivity, 1040 S cm^{-1}, is found at 300 °C for the composition x = 0.4. The ASR of the PSCF–GDC (50:50 by weight) cathode is as low as 0.046 Ω cm² at 800 °C. The values of the power densities are 520 mA cm^{-2}, 435 mW cm^{-2} and 303 mW cm^{-2} at 800 °C, 750 °C and 700 °C, respectively. All these results prove that PSCF-GDC (50:50 by weight) is a promising cathode material for IT-SOFCs.

Acknowledgements

This work was supported by the Natural Science Foundation of China (No. 10604020) and Jilin University.

References

[1] H.Y. Tu, Y. Takeda, N. Imanishi, O. Yamamoto, Solid State Ionics 117 (1999) 277–281.
[2] N.P. Brandon, S. Skinner, B.C.H. Steele, Annu. Rev. Mater. Res. 33 (2003) 183–213.
[3] K.T. Lee, A. Manthiram, Solid State Ionics 176 (2005) 1521–1527.
[4] B.C.H. Steele, Solid State Ionics 129 (2000) 95–110.
[5] Y. Jiang, S.Z. Wang, Y.H. Zhang, J.W. Yan, W.Z. Li, Solid State Ionics 110 (1998) 111–119.
[6] B. Morel, R. Roberge, S. Savoie, T.W. Napporn, M. Meunier, Appl. Catal. A: Gen. 323 (2007) 181–187.
[7] R. Doshi, V.L. Richards, J.D. Carter, X.P. Wang, M. Krumpelt, J. Electrochem. Soc. 146 (4) (1999) 1273–1278.
[8] S.J. Skinner, Int. J. Inorg. Mater. 3 (2001) 113–121.
[9] E. Boehm, J.-M. Bassat, M.C. Steil, P. Dordor, F. Mauvy, J.-C. Grenier, Solid State Sci. 5 (2003) 973–981.

[10] C.J. Fu, K. Sun, N.Q. Zhang, X.B. Chen, D.R. Zhou, Electrochim. Acta 52 (2007) 4589–4594.
[11] L.-W. Tai, M.M. Nasrallah, H.U. Anderson, D.M. Sparlin, S.R. Sehlin, Solid State Ionics 76 (1995) 259–271.
[12] T. Ishihara, M. Honda, T. Shibayama, H. Minami, H. Nishiguchi, Y. Takita, J. Electrochem. Soc. 145 (1998) 3177–3183.
[13] E.P. Murray, S.A. Barnett, Solid State Ionics 143 (2001) 265–273.
[14] K.T. Lee, A. Manthiram, J. Electrochem. Soc. 152 (1) (2005) A197–A204.
[15] H. Ullmann, N. Trofimenko, F. Tietz, D. Stöver, A. Ahmad-Khanlou, Solid State Ionics 138 (2000) 79–90.
[16] J.-H. Wan, J.-Q. Yan, J.B. Goodenough, J. Electrochem. Soc. 152 (2005) A1511–A1515.
[17] T. Ishihara, T. Kudo, H. Matsuda, Y. Takita, J. Electrochem. Soc. 142 (1995) 1519–1524.
[18] S. Kim, S. Wang, X. Chen, Y.L. Yang, N. Wu, A. Ignatiev, A.J. Jacobson, B. Abeles, J. Electrochem. Soc. 147 (2000) 2398–2406.